

# Neutron inelastic scattering of $^{232}\text{Th}$ : measurements and beyond

Eliot Party<sup>1,\*</sup>, Catalin Borcea<sup>2</sup>, Philippe Dessagne<sup>1</sup>, Xavier Doligez<sup>3</sup>, Grégoire Henning<sup>1</sup>, Maëlle Kerveno<sup>1</sup>, Alexandru Negret<sup>2</sup>, Markus Nyman<sup>4</sup>, Adina Olacel<sup>2</sup>, and Arjan Plompen<sup>4</sup>

<sup>1</sup>Université de Strasbourg, CNRS, IPHC UMR 7178, F-67000 Strasbourg, France

<sup>2</sup>Horia Hulubei National Institute for Physics and Nuclear Engineering (IFIN-HH), Reactorului 30, Magurele – Bucharest, 077125, Romania

<sup>3</sup>Institut de Physique Nucléaire, CNRS-IN2P3, Univ. Paris-Sud, Université Paris-Saclay, 91406 Orsay Cedex, France

<sup>4</sup>European Commission, Joint Research Centre, Directorate G – Nuclear Safety and Security, Unit G.2, Retieseweg 111, 2440 Geel, Belgium

**Abstract.** Gamma production cross sections have been obtained for 81 transitions in  $^{232}\text{Th}$  from  $(n,n'\gamma)$ , 11 in  $^{231}\text{Th}$  from  $(n,2n\gamma)$  and 7 in  $^{230}\text{Th}$  from  $(n,3n\gamma)$  reactions using prompt gamma spectroscopy. Incident neutron energies were determined using the neutron time-of-flight technique. Sources of uncertainty have been examined and their correlations have been computed. Total uncertainty on cross sections ranges from 4 to 20%. Obtained cross sections are in agreement with prior experiments, but are not well reproduced by the TALYS-1.8 reaction code using default parameters. During analysis, discrepancies between our findings and the Evaluated Nuclear Structure Data File (ENSDF) were noted. Future work related to the present experiment includes: improving theoretical models, quantifying the influence of the  $^{232}\text{Th}$  inelastic neutron cross section on reactor core parameters, and conducting additional measurements.

## 1 Introduction

Today, the lack of precision in nuclear data affects our capability to predict accurately some phenomena in nuclear reactors. For example, inelastic scattering off  $^{238}\text{U}$  is the main source of uncertainty due to nuclear data in power distribution of large reactor [1]. To answer to the need of lower uncertainties in nuclear data for applications, new precise measurements of cross sections are necessary.

In this paper, measurements of neutron inelastic scattering off  $^{232}\text{Th}$  using prompt gamma spectroscopy are presented.  $^{232}\text{Th}$  is an alternative nuclear fuel using the  $^{232}\text{Th}/^{233}\text{U}$  cycle. Inelastic scattering off  $^{232}\text{Th}$  may play the same role in this fuel as the one off  $^{238}\text{U}$  in usual fuel. Cross section measurements referenced in the EXFOR database [2], are mostly anterior to 1990, and used mainly direct neutron detection. Two studies used gamma spectroscopy to determine partial cross sections in 1980's, one by Dave et al. [3], the other by Filatenkov et al. [4]. Only a few of these measurements, and none using gamma detection, extended beyond 3 MeV in incident neutron energy, as shown on Fig. 1. This work provides new and precise measurements on a range of incident neutron energy extending to 20 MeV.

\*e-mail: [eliot.party@etu.unistra.fr](mailto:eliot.party@etu.unistra.fr)

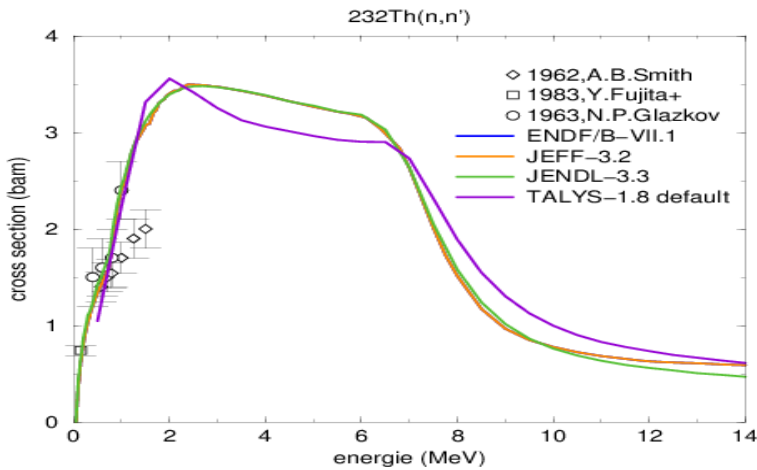


**Figure 1.** (color online) Previous experimental and evaluated data of the total inelastic neutron scattering cross section of  $^{232}\text{Th}$ .

## 2 Method used and experimental setup

To study inelastic neutron scattering off  $^{232}\text{Th}$  we detected  $\gamma$ -rays emitted by the deexciting  $^{232}\text{Th}$  nuclei, coupled with the time-of-flight technique, in which the incident neutron energy is deduced from the known distance to the neutron source and the measured flight time. This method can be used for all reactions where a gamma ray is emitted, such as the (n,2n) and (n,3n) reactions. Reactions producing one specific gamma transition from a residual nucleus, after emission of  $x$  neutrons, will be called (n,xn $\gamma$ ) reactions in the following. The goal is to obtain angle-integrated (n,xn $\gamma$ ) reaction cross sections for as many transitions as possible, on a neutron energy range pertinent to reactor applications.

Neutron source used was GELINA (Geel Electron LINear Accelerator) [5], operated by the European Commission Joint Research Centre (JRC) in Geel, Belgium. It generates neutron bursts at 800 Hz frequency by colliding electron pulses from the accelerator on a uranium target, where neutrons are produced by bremsstrahlung-induced reactions. Both moderated and unmoderated neutron beams are available on several flight paths of different lengths. The unmoderated neutron spectrum used in the present experiment is similar to the fission neutron spectrum in a nuclear reactor.

Our experimental setup, named GRAPhEME (GeRmanium Array for Actinides PrEcise MEasurements) [6] is placed at the 30 meter station of flight path 16. The time of flight range of interest spreads from 0.5 to 6 microseconds, corresponding to neutron energies from 20 MeV to 100 keV, respectively.

$\gamma$ -rays are detected using 4 planar HPGe counters placed at  $110^\circ$  and  $150^\circ$  from beam axis. Incident neutrons are monitored using a Fission Chamber (FC) containing  $^{235}\text{U}$  foils installed upstream of the target. Output signals from the detectors are processed by TNT-2 100 MHz digital acquisition cards. Measurements have been conducted over three campaigns in 2009, 2010 and 2013, totalling 800 hours of beam time. Only events within  $10\ \mu\text{s}$  before to  $50\ \mu\text{s}$  after a neutron pulse emission, are registered, storing the instant of detection and the signal amplitude. This large time gate allows observation of background radiation. HPGe counters are set to observe  $\gamma$ -rays of low energy, with a maximum efficiency for energies between 150 and 200 keV.

### 3 Analysis

#### 3.1 Data extraction

In order to determine the number of events in the fission chamber and the HPGe counters as a function of neutron time of flight, the data are sorted into two-dimensional time vs. energy histograms (as Fig. 2).

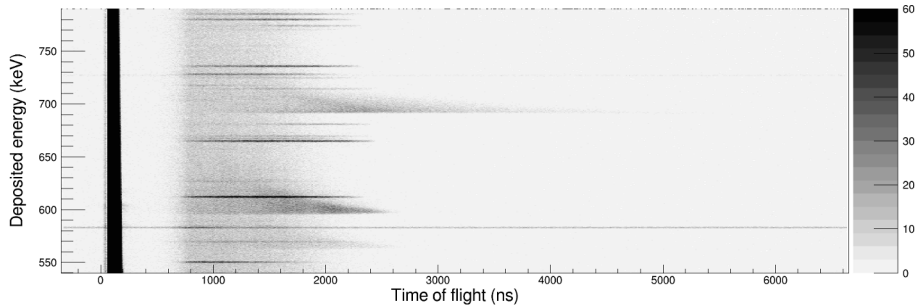


**Figure 2.** An example of a time-of-flight vs. deposited energy matrix, from data collected with one of the GRAPhEME HPGe detectors.

Before a neutron pulse emission, only background events are observed, mainly from  $^{235}\text{U}$  foil alpha radioactivity in FC, and  $^{232}\text{Th}$  target radioactivity  $\gamma$ -rays. This background is constant and present at every time. Then events caused by the bremsstrahlung radiation produced in the primary target are detected. The bremsstrahlung produces only some photofission in the FC, but their scattering by the  $^{232}\text{Th}$  target makes up 95% of events in HPGe counters, and induces significant pile up. After about 500 ns time-of-flight, corresponding to an incident neutron energy of 20 MeV, the first neutron-induced  $\gamma$ -rays are detected. As time passes, few neutrons reach target anymore, and only background is detected until the next neutron pulse.

In HPGe counters, we observe a smooth background and well resolved peaks in energy, present on a limited time of flight range. These peaks are identified with a transition in an isotope using mainly their centroid energy. If needed, their time range of presence and their area may act as hints. For peaks originating from (n,xn $\gamma$ ) reactions, area under peak  $N_\gamma$  on each HPGe counter is obtained for each neutron energy (time of flight) bin. Correction factor  $\tau_{pup}$  accounting for pile-up is computed using acquisition cards tagging of pile-up events. And the counter efficiency  $\epsilon_\gamma$  at given gamma energy is computed by MCNP [7], and verified using calibrated  $^{152}\text{Eu}$  source.

Number of incident neutrons impinging on the target for the same neutron energy bin is obtained using the number of fission events  $N_{fiss}$  detected in the corresponding time-of-flight bin. Other terms include  $^{235}\text{U}$  foil atomic density per unit area  $\zeta_{^{235}\text{U}}$ ,  $^{235}\text{U}$  standard fission cross section  $\sigma_{f,^{235}\text{U}}$  from reference [8], as well as FC detection efficiency  $\epsilon_{FC}$  and correction factor  $\tau_{att}$  for beam attenuation between FC and  $^{232}\text{Th}$  target [9]. Multiple scattering do not need to be corrected as thin target was used.

Then, for each energy bin, the angle-differential (n,xn $\gamma$ ) cross section is given by equation (1), with  $\zeta_{Th}$  being target atomic density per unit area.

$$\frac{d^2\sigma_{(n,xn\gamma)}}{dE d\theta}(E_n) = \frac{N_\gamma(E_n) \tau_{pup} \sigma_{f,^{235}\text{U}}(E_n) \epsilon_{FC} \zeta_{^{235}\text{U}}}{\zeta_{Th} \epsilon_\gamma N_{fiss}(E_n) \tau_{att}} \quad (1)$$

Choice of neutron energy bins is a compromise between neutron energy resolution and an increased uncertainty on the cross section caused by reduced statistics in smaller bins.

### 3.2 Covariances

To combine measurements of all detectors and to propagate the uncertainties, we need to compute covariances. Covariances of cross sections are obtained from covariances of each nine factors in Eq. (1) using uncertainty propagation in linear approximation. As some factors values are common to all energy bins (like target density  $\zeta_{Th}$ ), positive correlation is induced. A correlation matrix obtained for the 681 keV  $(n, n'\gamma)$  cross section is shown in Fig. 3. Only positive correlations are present, so the color palette ranges from 0 to 1. There are positive correlations between the cross section values over the neutron energy range covered here. Such a positive correlation between different neutron energies implies a lower uncertainty on the shape of the cross section than if no correlation was assumed. Thus, adequate treatment of covariances is necessary for the correct use of our results, for example in an evaluation.

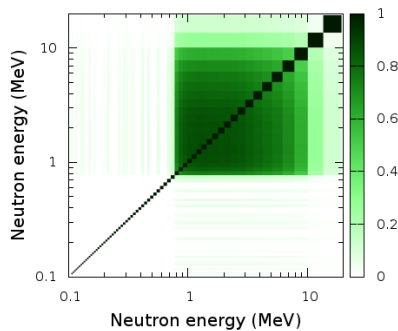


**Figure 3.** (color online) Correlation matrix of the measured 681 keV  $(n, n'\gamma)$  cross section.

## 4 Results

### 4.1 Some remarks on the measured cross sections

81 cross sections from  $^{232}\text{Th}(n, n'\gamma)$  reactions have been extracted. Additionally 11  $^{232}\text{Th}(n, 2n\gamma)^{231}\text{Th}$  and 7  $^{232}\text{Th}(n, 3n\gamma)^{230}\text{Th}$  cross sections have been obtained. For 28 out of the 30 lowest lying excited states of  $^{232}\text{Th}$ , at least one deexciting transition was observed and its  $\gamma$ -ray production cross section measured. The remaining two were weakly populated due to their high spins ( $7^+$  and  $12^+$ ). Four  $(n, n'\gamma)$  cross sections are shown in Fig. 4. The two on the left are the 49 keV transition from  $2^+$  state and the 223 keV transition from  $8^+$  state of ground state band, and the two on the right are from other bands head states. Main component of the total uncertainty of the cross section is either statistics or detection efficiencies, depending on the transition. Efficiencies and other systematic uncertainties result in a correlated uncertainty of 3.5% on the measured cross sections. Best precision obtained is 4% for the measured  $(n, n'\gamma)$  cross sections.

A large number of  $(n, n'\gamma)$  cross sections had been published by Dave et al. (1985) [3], while other studies only published deduced level population cross section. As Dave et al. measurements only extend up to 2.2 MeV, energy ranges in Fig. 4 have been reduced to 10 MeV to ease comparison. Our results are in good agreement: from the 57 cross sections measured in both experiments (no transitions below 550 keV in Dave et al.), only 5 show significant differences, but they are weakly populated or are contaminated by nearby peaks.

Obtained cross sections have also been compared with predictions of the reaction code TALYS 1.8 [10], using the default calculation parameters. Differences are observed in shape or in magnitude for most cross sections. They may be explained to some extent by incomplete nuclear structure knowledge, such as unknown spins, parities, or branching ratios, which can lead to over- or under-estimation of the cross section in TALYS calculations.

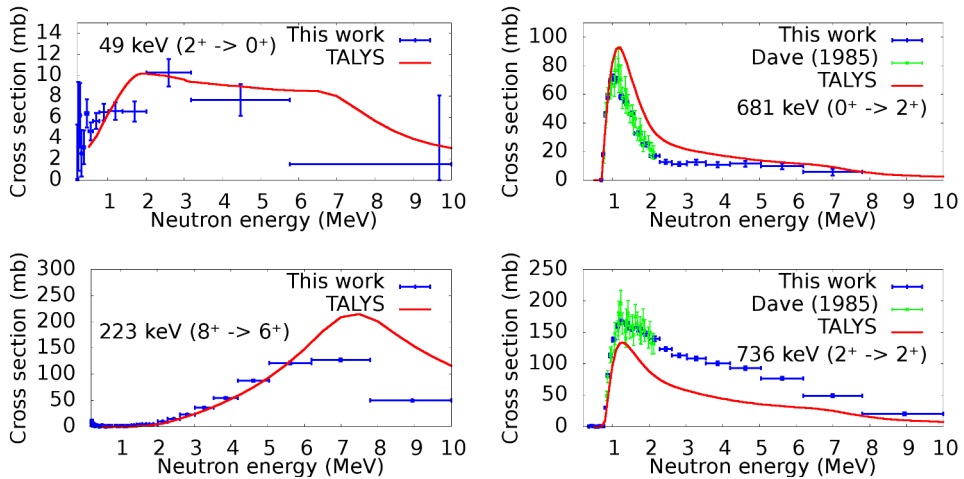


**Figure 4.** (color online) The  $(n,n'\gamma)$  cross sections are chosen as representative of shapes observed. This work is compared with Dave et al. [3] and predictions of TALYS-1.8 with default parameters.

## 4.2 Shortcomings in the nuclear structure knowledge

Some discrepancies in the ENSDF [11] nuclear structure database were found during data analysis. First, we found an erroneous Relative Intensity (RI in the following) in ENSDF for the level  $7^-$  at 1043 keV in  $^{232}\text{Th}$ . 486 keV and 159 keV transitions from this level are reported with RIs of 65 and 100 respectively. Yet, our measurements suggests RIs of 100 and 18.5(30). Indeed, RIs of 4.5 and 6.9 (relative to another transition) in Nuclear Data Sheets [12] were instead reported to be 45 and 6.9 in original reference [13], equivalent to RIs of 100 and 15.3. The original values are compatible with our measurements.

Second, there are ten levels in ENSDF for which at least one  $\gamma$ -ray observed in our measurement has an unknown RI. Yet, these are not necessarily weak. For the 1121 keV( $2^+$ ) level of  $^{232}\text{Th}$ , while RI are only reported for transitions at 959, 407 and 347 keV as 100%, 37% and 30%, our measurement suggests RI of 300% (relative to 959 keV transition) for the 1072 keV transition. Other studies [14–16] confirm the high RI for the 1072 keV transition.

Finally, new levels and transitions for  $^{232}\text{Th}$  were proposed by Demidov et al. (2008) [16]. Some of these transitions were observed in our measurements, in particular a strong transition at 1075.5 keV included in our results. This recent proposition, as well as uncertain spin-parity assignments, shows that the level scheme of  $^{232}\text{Th}$  is not definitive at high excitation energies covered in our measurement.

Our study uses nuclear structure, both in analysis, as  $\gamma$ -rays are identified from transitions registered in ENSDF or XUNDL [11] (eXperimental Unevaluated Nuclear Data List), and in theoretical interpretation, as prediction from theory is affected by deexcitation paths. Consequently, these shortcomings interfere with our study and improved knowledge of the  $^{232}\text{Th}$  level scheme is required.

## 5 Outlook of related activities

### 5.1 Collaboration on theory

To obtain cross sections pertinent to reactor applications, like the total  $(n,n')$  cross section, only from the  $(n,xn\gamma)$  cross sections is not possible if all deexcitation paths are not observed.

Our approach is to use theoretical models constrained with experimental values in order to fill the gaps. This work is done in collaboration with theoreticians from CEA (Commissariat à l’Energie Atomique et aux énergies alternatives). Collaboration on the  $^{232}\text{Th}$  cross section is only beginning, but results have already been obtained on  $^{238}\text{U}$  [18]. This paper points that adjustment of theory parameters (spin distribution, gamma strength...) could reproduce several features observed in measurements. For example, adjustment of the spin distribution from an ad hoc exciton model to a QRPA calculated distribution enabled a better agreement with measurement, especially for transitions in the ground state band. The measured  $^{232}\text{Th}(n,xn\gamma)$  cross sections should put further constraints on the models.

## 5.2 Sensitivity studies

To quantify the influence on reactors of inelastic scattering of  $^{232}\text{Th}$ , compared to other cross-sections, it was decided to propagate uncertainties and to calculate sensitivity on three different parameters of nuclear reactors (neutron multiplication factor  $k_{eff}$ , delayed neutron fraction  $\beta_{eff}$  and radial power distribution  $P(r)$ ). Recent developments in the Monte-Carlo transport codes MCNP [7] and SERPENT [19] allow sensitivity calculations of  $k_{eff}$  to nuclear data thanks to the generalized perturbation theory. Then, from those sensitivity coefficients, it is possible to calculate uncertainties if the covariance matrix of nuclear data used is known. On the other hand, the Total Monte Carlo method (TMC) [20] consists in sampling randomly nuclear parameters in order to build, for one isotope of interest, hundreds of evaluated cross section file from TENDL [21]. The sampling is made to be representative of uncertainties on nuclear data. Then a MCNP or SERPENT calculation is performed for each file from this library of nuclear data and the distribution of calculated parameters gives directly the uncertainty due to the nuclear data of one particular isotope.

These methods were applied to a Pressurized Water Reactor fueled with a  $^{232}\text{Th}/^{233}\text{U}$  fuel. The TMC method applied for  $k_{eff}$  calculations gave uncertainties up to 6%, justifying the strong needs of improvement for thorium cross sections. We took the opportunity of TENDL to build covariance matrices for  $^{232}\text{Th}$  and  $^{233}\text{U}$  cross-section for several energy binning. We combined them with the sensitivity coefficients calculated with SERPENT and MCNP to compare the perturbation theory with the TMC method. We showed that a high number of energy bins for the covariance matrix is necessary to obtain results in perfect agreement. This condition allows us to reduce drastically the huge computational power needed for the TMC and we proved that reliable covariance of nuclear data may be obtained with TENDL. Further studies are ongoing for  $\beta_{eff}$  and  $P(r)$  on other reactor types, including sodium cooled reactors for fast neutron spectrum.

## 5.3 Experimental developments

The GRAPhEME spectrometer is continuously being upgraded. It has been used for ten years to measure  $(n,xn\gamma)$  cross sections on several isotopes. HPGe counters have been added in 2014 (one being segmented to overcome difficulties induced by very high activity isotopes  $^{233}\text{U}$  and  $^{239}\text{Pu}$ ) and in 2018 the acquisition system has been changed to the FASTER system [22].

Apart from this gradual evolution, we plan to adress one of the problems of gamma spectroscopy: unobserved level deexcitation by internal conversion. As an example, 99.7% of deexcitation of the  $^{232}\text{Th}$  first excited level at 49 keV occurs by internal conversion, decreasing a prominent 3 b deexcitation cross section to a barely detectable 10 mb gamma emission cross section, with consequent uncertainties (see Fig. 4 upper left corner). Tests for a proof of concept of DELCO (for Detecteur d’ELectron de CONversion), a new detection setup aiming

at detecting conversion electrons using silicon detectors, have been started. If its completion is successful, it will allow the detection of deexcitation paths still unobserved in our experiment.

As lack of nuclear structure information for some isotopes affects the interpretation of our measurements, it would also be of interest to perform nuclear structure measurements on the isotopes concerned, primarily  $^{238}\text{U}$ . This could be carried out by coupling GRAPhEME with GAINS [23, 24], another HPGe spectrometer in our experimental collaboration.

## 6 Conclusion

The main result of this work is the measurement of 81  $^{232}\text{Th}(n,n'\gamma)$  cross sections, on a large incident neutron energy range, up to 20 MeV. These cross sections show and cover the deexcitation of most low-lying levels. Covariances associated to each cross section have been derived to ensure their correct uses. The present measurement is a significant improvement from preceding measurements by other teams, in which the incident neutron energy did not exceed 3 MeV, the uncertainties were higher and first transitions in the ground state band were not reported. Upcoming work will include the integration of measured cross section in EXFOR, as well as collaboration to derive theoretical interpretation, sensitivity studies in reactor applications, and development of new equipment to account for conversion electrons.

## References

- [1] M. Salvatores et al., International Evaluation Co-operation Vol. 26, NEA No .6410 (2008)
- [2] V. Zerkin et al., Nucl. Instrum. Methods A **888**, p. 31 (2018)
- [3] J.H. Dave et al., Nuclear Science and Engineering **91**, p. 187 (1985)
- [4] A.A. Filatenkov et al., USSR report to the I.N.D.C. **298**, p. 63 (1989)
- [5] D. Ene et al., Nucl. Instrum. Methods A **618**, p. 54 (2010)
- [6] M. Kerveno et al., European Physical Journal A **51**:167, p. 1-18 (2015)
- [7] J.T. Goorley et al., Initial MCNP6 Release Overview - MCNP6 version 1.0 , LANL, LA-UR-13-22934 (2013)
- [8] A.D. Carlson et al., Nucl. Data Sheets **148**, p. 143-188 (2018)
- [9] J.C. Thiry, Ph.D. thesis, Univ. de Strasbourg (2010), <http://scd-theses.u-strasbg.fr/2016/>
- [10] A.J. Koning et al., "TALYS-1.0" in Int. Conf. on Nuc. Data for Sci. and Tech., EDP Sciences, p. 211 (2008)
- [11] Evaluated Nuclear Structure Data File, available from <http://www.nndc.bnl.gov/ensdf>
- [12] E. Browne, Nucl. Data Sheets **107**, p. 2579 (2006)
- [13] C. Gunther et al., Phys. Rev. C **61**, 064602 (2000)
- [14] W.R. McMurray et al., Zeitschrift für Physik **253**, p. 289 (1972)
- [15] F.K. McGowan et al., Nuc. Phys. A**562**, p. 241 (1993)
- [16] A.M. Demidov et al., Phys. At. Nucl. **71**, p. 1839 (2008)
- [17] Experimental Unevaluated Nuclear Data List, available from [www.nndc.bnl.gov/xundl](http://www.nndc.bnl.gov/xundl)
- [18] M. Dupuis et al., European Physical Journal A **51**:168, p. 1-16 (2015)
- [19] J. Leppänen et al., Ann. Nuc. Energy **82**, p. 142-150, (2015)
- [20] D. Rochman et al., Ann. Nuc. Energy **38** p. 942-952 (2011)
- [21] A.J. Koning, D. Rochman, Nucl. Data Sheets **113** p. 2841- 2934 (2012)
- [22] FASTER project—IN2P3, available from: <http://faster.in2p3.fr/>
- [23] D. Deleanu et al., Nucl.Instrum. Methods A **624**, p. 130 (2010)
- [24] A. Negret et al., Nucl. Data Sheets **119**, p. 179 (2014)